Macromolecules

pubs.acs.org/Macromolecules Article

Simulated Osmotic Equation of State for Poly(ethylene Oxide) Solutions Predicts Tension-Induced Phase Separation

Wezi D. Mkandawire and Scott T. Milner*

Cite This: *Macromolecules* 2021, 54, 3613–3619 Read Online

ACCESS | Metrics & More | Article Recommendations

ABSTRACT: Poly(ethylene oxide) (PEO) is soluble in water, but its solubility is sensitive to changes in temperature, pressure, and stress. Notably, phase separation can occur when PEO solutions are subjected to strong flow. To explore these phenomena, we use molecular dynamics simulations to examine the phase behavior of PEO under tension in aqueous solution by pulling on the ends of each chain. At the same time, we impose a harmonic potential on the chains, resulting in a nonuniform concentration profile. We analyze this concentration profile to obtain the osmotic pressure versus concentration. Comparing this result to the osmotic pressure prediction from the Flory–Huggins free energy, we obtain the chi parameter χ for PEO in water as a function of volume fraction ϕ and chain tension. We observe an increase in $\chi(\phi)$ as the tension increases and a moderate increase in χ as the polymer volume fraction ϕ increases, consistent with experimental observations.

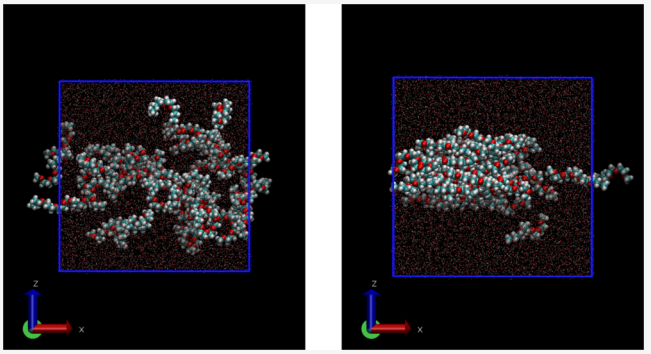

INTRODUCTION

Poly(ethylene oxide) (PEO) is a hydrosoluble polymer with numerous medical, biochemical, and industrial benefits.[1,2] Recently, PEO has garnered attention because of its interesting phase behavior under flow: when PEO solutions are placed in strong shear flow, the solvent quality apparently worsens, and the polymer ultimately falls out of solution.[3]

PEO, with a repeating unit of $O-CH_2-CH_2$, can be divided into two segments: hydrophobic carbons and hydrophilic oxygens. The oxygens form hydrogen bonds, resulting in solubility of PEO in water. However, under increasing pressure, temperature, and stress, these hydrogen bonds diminish, and PEO–water interactions become less favorable.[4]

Theoretical phase diagrams and experimental data show that PEO solubility depends on temperature, pressure, and concentration.[5] PEO in water exhibits a reentrant phase diagram and remains as a single-phase solution between lower and upper critical temperatures.[5] Outside of this temperature range, PEO falls out of solution. This behavior is characteristic of many hydrogen-bonding polymers.

Although most studies of PEO solubility focus on the temperature effects, its solubility depends on polymer concentration as well. Polymer–solvent interactions are typically represented in terms of the Flory χ parameter, which phenomenologically may be regarded as a function of both temperature and concentration, $\chi(T, \phi)$.

Bae and co-workers measure changes in the PEO χ parameter as concentration increases.[6] Holding a PEO solution at constant temperatures and pressures, they gradually increase the solvent weight fraction, effectively decreasing the polymer concentration. As the polymer concentration decreases, the χ parameter decreases, corresponding to an increase in solvent quality. Conversely, the solvent quality worsens with an increase in PEO concentration.

Previous simulations focus on how hydrogen bonding affects PEO solubility in water. Smith and co-workers look at how concentration influences the ability of PEO to hydrogen-bond.[7] From pair distribution functions of oxygens on PEO in water with water hydrogens, they estimate the likelihood of water–water and PEO–water hydrogen bonding at different polymer concentrations. The probability of finding PEO oxygens and water hydrogens close enough to form hydrogen bonds drops significantly with increasing concentration.

Sommer and Donets explore strain-induced phase separation of PEO in water, examining how chain tension affects hydrogen bonding and polymer conformation.[8] In their work, they apply equal and opposite forces on the chain ends of up to 350 pN, which is large enough to force the chains

Received: October 14, 2020
Revised: March 9, 2021
Published: April 6, 2021

https://doi.org/10.1021/acs.macromol.0c02334
Macromolecules 2021, 54, 3613–3619

to essentially all-trans configurations. The chains become parallel and straight and readily crystallize in the simulation under the action of dispersion interactions. These applied forces are well in excess of the characteristic force $F_c = k_bT/L_k$ (where L_k is the Kuhn length), which is around 4 pN for PEO. At this tension, Kuhn steps are slightly biased in the direction of the force, and chains begin to align significantly.

In this work, we investigate flow-induced phase separation of PEO solutions using a new method. Like Sommer and Donets, we pull on the ends of the polymer chains to explore flow-induced strain without conducting a flow simulation, albeit at much lower and more realistic tension values. However, rather than quantifying tension effects through counting hydrogen bonds, we adapt a recently developed simulation method[9] for measuring the osmotic pressure versus concentration for salt solutions to obtain $\chi(\phi)$ for PEO in water.

In the new method, we impose a harmonic confining potential and thereby produce nonuniform concentration profiles of PEO. Analyzing the balance of forces on the polymers, we compute the osmotic pressure Π across the system, from which we obtain $\Pi(\phi)$. Comparing this osmotic pressure to that predicted by the Flory–Huggins free energy, we extract the χ parameter as a function of ϕ for each applied tension F. The resulting family of curves $\chi(\phi, F)$ shows that the water–polymer interactions become unfavorable as the tension on the chains increases.

OSMOTIC PRESSURE AND MISCIBILITY

Placing the PEO chains in a harmonic potential $U(z)$ induces a nonuniform equilibrium concentration profile of approximately Gaussian shape. If the PEO chains behaved as an ideal gas, the concentration profile would be exactly Gaussian, proportional to $e^{-\beta U(z)}$. The concentration profile emerges from the balance between the force F_U exerted by the imposed potential $U(z)$ and the force F_Π exerted by the osmotic pressure $\Pi(z)$. For a thin slab of solution from z to $z + \Delta z$, we find F_U and F_Π as

$$F_U = \phi(z)\frac{dU(z)}{dz}\Delta z \tag{1}$$

$$F_\Pi = \frac{d\Pi(z)}{dz}\Delta z \tag{2}$$

The force balance implies the relation

$$\frac{d\Pi(z)}{dz} = -\phi(z)\frac{dU(z)}{dz} \tag{3}$$

By discretizing the force balance, writing the potential $U(z)$ as $U = 1/2Kz^2$, and averaging ϕ and z across individual slabs, we find an expression for the osmotic pressure difference across the slabs

$$\Pi_2 = \Pi_1 + \frac{\phi_2 + \phi_1}{2}\frac{z_2 + z_1}{2}K\Delta z \tag{4}$$

We assume the osmotic pressure is ideal at the simulation boundaries, where the concentration approaches zero and $\Pi = ckT$, where c is the chain concentration. This allows us to compute the osmotic pressure from the edges of the simulation box to the center. Finally, $\Pi(z)$ and $\phi(z)$ can be combined to obtain $\Pi(\phi)$.

The osmotic pressure for a polymer solution can be predicted from the Flory–Huggins free energy.[10] Comparing this prediction to the observed $\Pi(\phi)$, the function $\chi(\phi)$ can be fit to the data. The Flory–Huggins free energy per unit volume f takes the form

$$v_0\beta f = \left(\frac{\phi}{N}\right)\log\phi + (1-\phi)\log(1-\phi) + \chi\phi(1-\phi) \tag{5}$$

for a chain of N monomers of volume v_0 (and a solvent molecule of equal volume). The osmotic pressure Π is related to the chemical potential by

$$v_0\Pi = \mu_s^* - \mu_s \tag{6}$$

where μ_s^* is the chemical potential of pure water and μ_s is the chemical potential of water in solution. Equation 6 says that the change in free energy $\mu_s^* - \mu_s$ to transfer a water molecule from pure water to the solution is equal to the thermodynamic work done against osmotic pressure $v_0\Pi$ to make room for the transferred molecule.

The solvent chemical potential in an incompressible solution can be obtained from $f(\phi)$ as

$$\mu_s = v_0(f - \phi f'(\phi)) \tag{7}$$

Applying this expression to the Flory–Huggins free energy, we obtain the Flory–Huggins expression for osmotic pressure

$$\beta v_0\Pi = \left(\frac{\phi}{N}\right) - (\phi + \log(1-\phi) + \chi\phi^2) \tag{8}$$

The first term in eq 8 represents the ideal gas limit, $\Pi = k_bT\phi/(v_0N)$. Expanding the second term for a small ϕ, we obtain $1/2(1-2\chi)\phi^2$, which gives the second virial coefficient to $\Pi(\phi)$.

The Flory–Huggins χ parameter quantifies enthalpic polymer–solvent interactions and governs solubility. χ values up to 0.5 correspond to good solvents. For χ above 0.5, the $O(\phi^2)$ contribution to $\Pi(\phi)$ becomes negative, marking the onset of poor solvent behavior.

Simulation Setup. For our osmotic pressure simulations, we use rather short chains so that the dynamics is as rapid as possible. We choose chains that are about twice the Kuhn length (approximately 1.1 nm for PEO), which ensures that the chains are flexible.

Our simulations consist of 40 PEO chains with the formula $CH_3–(O–CH_2–CH_2)_5–O–CH_3$ and 6359 water molecules. The system box measures 6 nm on each side. All jobs are run using GROMACS with OPLS-AA potentials. Our simulations run on eight processor cores on a single node, with a time step of 2 fs at a rate of around 80 ns/day.

Typical simulation snapshots are shown in Figure 1, taken using VMD.[11] The chains are pulled in the (red) x direction, while the confining potential is imposed in the (blue) z direction.

To pull the chains to the center of our box, we use GROMACS "pull code" options to impose a harmonic potential on every PEO oxygen. To impose such a potential, every pull group must be defined in a system index (.ndx) file; for each group, pull options are then included in the molecular dynamics parameters (.mdp) file. These lengthy and repetitive instructions are generated using bash scripts; examples of individual entries are given in the Appendix, Table 1.

By imposing a harmonic potential $U(z) = 1/2Kz^2$, we ensure that the nonuniform concentration profile spans a wide range of values. Specifically, we choose K such that the energy difference between the middle of the box and the boundary is

https://doi.org/10.1021/acs.macromol.0c02334
Macromolecules 2021, 54, 3613–3619

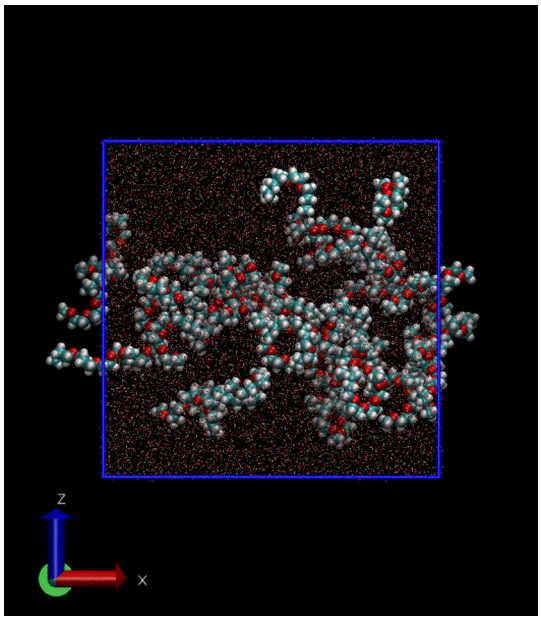

Figure 1. VMD snapshot at a tension of 0 kJ/mol/nm.

Table 1. Harmonic Potential Pull Code Instructions

```
pull = yes
pull-nstfout = 100; 0.1 ps
pull-nstxout = 100; 0.1 ps
pull-ngroups = 320
pull-ncoords = 320
pull-group1-name = PEOo1
pull-coord1-type = umbrella
pull-coord1-geometry = direction-periodic
pull-coord1-vec = 0 0 1
pull-coord1-groups = 0 1
pull-coord1-origin = 3. 3. 3.
pull-coord1-dim = N N Y
pull-coord1-k = 0.3696
pull-group2-name = PEOo2
```

$4k_bT$ so that the concentration at the system boundaries is e^{-4} times the maximum concentration. For our simulation box of 6 × 6 × 6 nm, we have

$$K = \frac{8k_bT}{9} \tag{9}$$

Since the potential acts on every oxygen atom and each chain contains six oxygens, we divide this value by six to get the spring constant k = 0.3696 kJ/mol/nm^2 on each oxygen, as shown in Table 1.

To place chains under tension, we apply equal and opposite forces on the ends of each chain and again use pull code options to impose a constant force (an example of these pull code options is given in the Appendix, Table 2). Pulling on the chain ends simulates the tension experienced by polymers when placed in strong flows. The larger the tension, the straighter the chains become, allowing us to observe the phase behavior of PEO in strained conditions. We imposed forces up to nearly 20 times the characteristic force $F_c = k_bT/L_k$ for PEO (equal to around 4 pN), which results in significantly but not fully extended chains.

Table 2. Pull Options for a Tension of 10 kJ/mol/nm in the + x Direction

```
pull-group241-name = PEOo1
pull-coord241-type = constant-force
pull-coord241-geometry = direction-periodic
pull-coord241-vec = 1 0 0
pull-coord241-groups = 0 1
pull-coord241-dim = Y N N
pull-coord241-k = 10
```

After energy minimization and equilibration, we ran simulations at tensions of 0, 10, 15, 20, 25, 30, 35, and 40 kJ/mol/nm. Each successive run starts with the final configuration of the previous run, roughly corresponding to a gradual increase in flow rate. Production simulations were run for 80 ns at each tension. As shown in the next section, this run length was sufficient to produce smooth and reliable concentration profiles from which osmotic pressures were obtained.

Simulation Results. As the tension increases, we observe the polymers increasingly concentrate in the middle of the box (see Figure 2). Figure 3 shows the corresponding stretching of the chains as the tension increases. While the chains do not become completely straight, we observe a significant change in their end-to-end length.

Evaluating the mean square end-to-end distance of all chains for each tension, we observe the chain lengths increase toward the fully extended chain length of roughly 2 nm (Figure 4). The chains are stretched substantially but not to their maximum length.

For each applied tension, we measure the time-averaged concentration as a function of z (distance from center). Averaging the concentration on opposite sides of the simulation box, we obtain the plots shown in Figure 5.

As the tension increases, the concentration becomes more peaked in the center, consistent with the clumping of polymers, as seen in the images of Figure 2. The concentration at the boundaries remains small for all tension values.

One potential concern with our method is that we impose a significant concentration variation over a rather short length scale and then model the resulting osmotic pressure profile with a free energy that neglects gradient terms. We have performed two tests to verify that our results are not spuriously affected by the small distance over which the harmonic potential and thus the concentration varies.

First, we have compared concentration profiles for chains without tension in a harmonic potential, for a system of the original size, and a system twice as wide in the confinement (z) direction with twice as many chains. The two simulations give identical concentration profiles when plotted versus reduced length z/L_z, which supports the assumption that effects of concentration gradients are small.

Second, we have simulated chains under tension with and without the harmonic potential applied and measured the same average chain dimensions in both simulations. This suggests that the harmonic potential does not interact with the chain entropic springs and that applying the potential does not compress the chain trajectories or make them easier to stretch.

Analysis. Equation 4 calculates the osmotic pressure Π from the concentration profile, which gives us the osmotic pressure as a function of concentration Π(c). To fit the osmotic equation of state to this data, we first convert

https://doi.org/10.1021/acs.macromol.0c02334
Macromolecules 2021, 54, 3613−3619

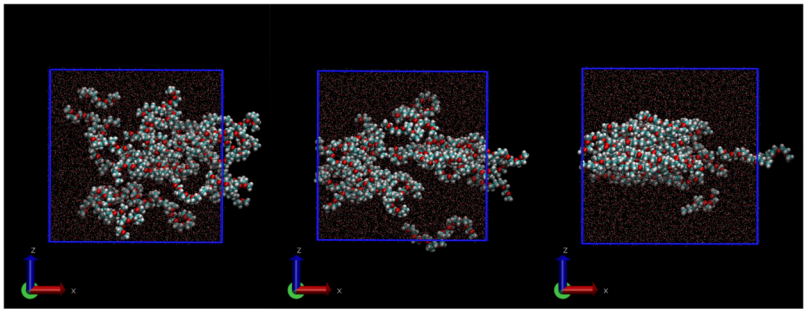

Figure 2. VMD snapshots of tensions 10, 20, and 40 kJ/mol/nm (from left to right).

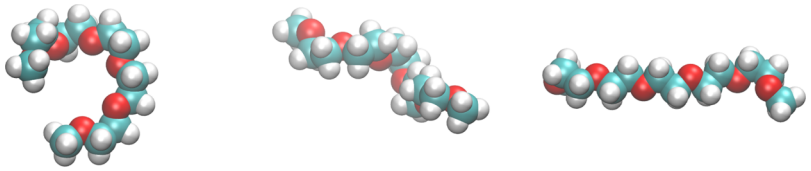

(a) (b) (c)

Figure 3. Typical configurations of single PEO chains at (a) 0, (b) 20, and (c) 40 kJ/mol/nm.

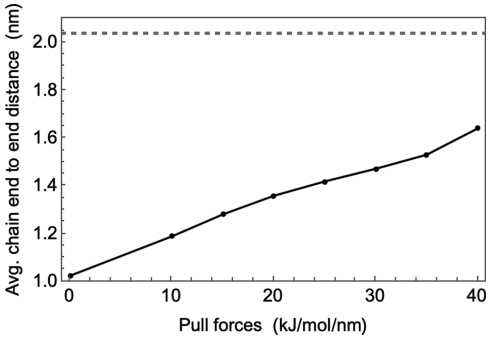

Figure 4. Average chain end-to-end distance vs pull force plot tensions of 0, 10, 15, 20, 25, 30, 35, and 40 kJ/mol/nm. Distances are 1.02, 1.19, 1.28, 1.36, 1.42, 1.47, 1.53, and 1.64 nm, respectively.

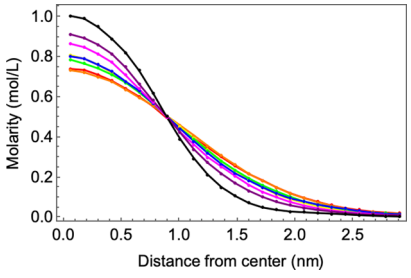

Figure 5. Concentration (mol/L) vs distance from center (nm) plot for tension values 0 (red), 10 (orange), 15 (yellow), 20 (green), 25 (blue), 30 (magenta), 35 (purple), 40 (black).

concentration c to volume fraction ϕ using the relationship $\phi = cNv_0$ to obtain the osmotic pressure as a function of volume fraction $\Pi(\phi)$ (Figure 6). Evidently, the osmotic pressure drops as the tension increases and rises as the volume fraction ϕ increases.

To extract the effective χ parameter as a function of ϕ and T, we fit the Flory osmotic equation of state in eq 8 onto our data to extract the χ parameter. We take v_0 to be the solvent volume, which ensures a reasonable entropic contribution to osmotic pressure in the limit of dilute solvent. Consequently,

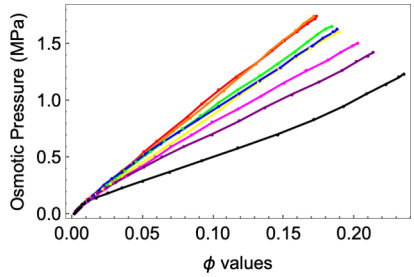

Figure 6. Osmotic pressure (MPa) vs ϕ value plot for tensions of 0 (red), 10 (orange), 15 (yellow), 20 (green), 25 (blue), 30 (magenta), 35 (purple), and 40 (black) kJ/mol/nm.

we set the number of monomers per chain to N such that $Nv_0 = v_c$, where v_c is the displaced volume of a chain. This gives $N = 13$ and ensures that the volume per chain is correctly represented.

To extract $\chi(\phi)$, we isolate the $\chi(\phi)\phi^2$ term in the osmotic equation of state. For an athermal solvent in which water and PEO experience no attractive or repulsive interactions ($\chi = 0$), the osmotic pressure would be

$$\beta v_0 \Pi_{\chi=0} = \left(\frac{\phi}{N}\right) - (\phi + \log(1-\phi)) \tag{10}$$

Subtracting the total osmotic pressure from the athermal osmotic pressure, we obtain

$$\chi(\phi) = \frac{\Pi_{\chi=0} - \Pi}{\phi^2} \tag{11}$$

The right-hand side of eq 11 produces data for $\chi(\phi)$ at varying tensions (Figure 7). After careful inspection of our original $\Pi(\phi)$ data, we drop some data points near the simulation boundaries where the concentration is small. These points fluctuate substantially and give specious results for $\chi(\phi)$ at low ϕ. Depending on the nature of the data for each tension, we drop around 7−10 points up to a volume fraction of around 0.02.

https://doi.org/10.1021/acs.macromol.0c02334
Macromolecules 2021, 54, 3613−3619

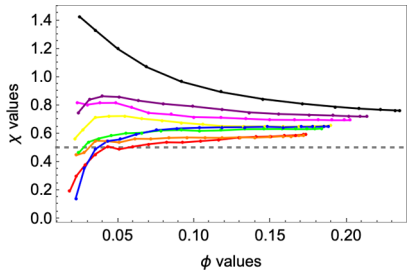

Figure 7. $\chi(\phi)$ vs ϕ values data for tensions of 0 (red), 10 (orange), 15 (yellow), 20 (green), 25 (blue), 30 (magenta), 35 (purple), and 40 (black) kJ/mol/nm before fitting. Dashed line at $\chi = 0.5$ represents the theta point at which phase separation begins.

To check our results for $\chi(\phi)$, we use it to compute the full osmotic pressure and compare the prediction with our original $\Pi(\phi)$ data (Figure 8). Figure 7 represents the resulting family of curves for χ as a function of volume fraction ϕ for each chain tension.

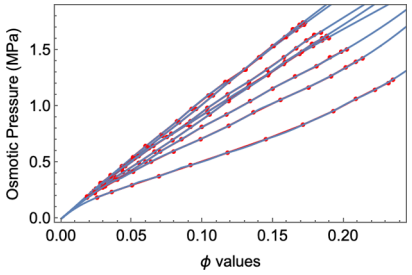

Figure 8. Osmotic pressure vs ϕ predicted from extracted $\chi(\phi)$ (blue) with the original osmotic pressure vs ϕ value data (red) for all tensions.

Two key observations are evident in Figure 7: (1) as the tension increases, $\chi(\phi)$ likewise increases, signifying the worsening of solvent quality. The effect becomes strong for forces of 30 pN or greater. (2) At all but the largest tensions, the solvent quality worsens as the volume fraction increases.

Structural Characterization. PEO solubility is influenced by the arrangement of water molecules surrounding the polymer chains. We can gain insight into why the PEO solution solvent quality worsens as chains are stretched or concentration increases by observing the number of hydrogen bonds.

To count hydrogen bonds, we run simulations of uniform systems at varying tensions. We use correlation functions to measure the probability of finding certain atoms close to one another. As tension increases, the number of hydrogen bonds decreases. Moreover, as tension increases, we observe a tendency for the PEO hydrocarbons to clump together, while PEO oxygens and water oxygens avoid each other, consistent with the onset of phase separation.

To identify hydrogen bonds,[12] we employ a criterion of distances and angles between the water oxygen, water hydrogen, and PEO oxygen, which serve as the donor (D), hydrogen (H), and acceptor (A), respectively. These groups must be within a distance $d(\mathrm{D-A}) \leq 3.0$ Å and an angle $\angle(\mathrm{D-H-A}) \leq 20°$ (an angle of 0° means all three atoms are in a straight line, as seen in Figure 9).

Hydrogen bonding identification is performed using VMD, analyzing simulations that use the same conditions as our previous jobs measuring osmotic pressure but without the confining potential at constant tensions of 0, 20, 30, and 40 kJ/mol/nm.

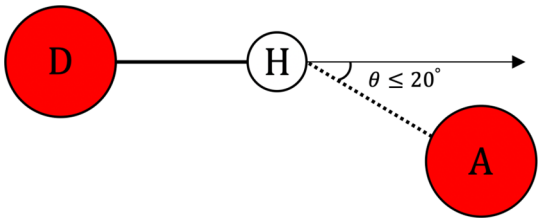

Figure 9. Example of the VMD hydrogen bonding angle criterion.

First, we measure the number of hydrogen bonds with water formed per PEO oxygen. As shown in Figure 10, PEO oxygens form a hydrogen bond around one-fourth of the time, with a smooth decrease in probability as the tension increases.

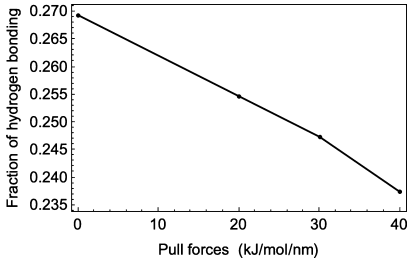

Figure 10. Fraction of hydrogen bonding vs tension.

Another way to assess the probability of PEO to form hydrogen bonds is by examining the radial distribution functions $g(r)$ between PEO oxygens and water oxygens. This $g(r)$ gives the likelihood of finding a water oxygen at a given distance from a PEO oxygen, relative to the average concentration of water oxygens.

We calculate the average number $\overline{n}$ of water oxygens within hydrogen bonding distance r from PEO oxygens by integrating $g(r)$ over a spherical shell

$$\overline{n} = c\int_0^r 4\pi r^2 g(r)\mathrm{d}r \tag{12}$$

where c is the average concentration of water oxygens. We find approximately 1.93, 1.84, 1.71, and 1.59 water oxygens within range of each PEO oxygen for the 0, 20, 30, and 40 kJ/mol/nm tensions, respectively. Evidently, only a fraction of these form hydrogen bonds by the geometric criterion we imposed. Quantitatively, we observe an 18% decrease in water oxygens within the hydrogen bonding distance, comparable to the observed 12% decrease in hydrogen bonding.

Note that both the hydrogen bond probability (Figure 10) and the number of water oxygens near a PEO oxygen (Figure 11) decrease steadily as tension increases, with no dramatic change as the phase boundary is approached. This suggests that the decreased formation of hydrogen bonds is a cause of phase separation, not a consequence of it.

Fewer hydrogen bonds lead to poor solvent behavior, which in turn leads to clumping of PEO hydrocarbons, which we again quantify with radial distribution functions. Specifically, we measure the pair distribution function from carbons on one given chain to carbons on all other chains. The result of averaging $g(r)$ over time and 10 different chains is shown in Figure 12 for tension values of 0, 20, 30, and 40 kJ/mol/nm.

https://doi.org/10.1021/acs.macromol.0c02334
Macromolecules 2021, 54, 3613−3619

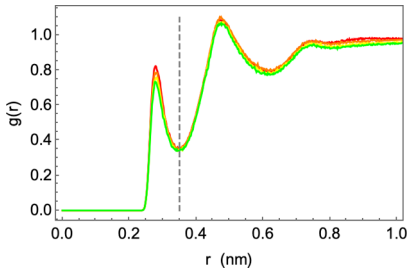

Figure 11. PEO oxygen to water oxygen $g(r)$ vs r (nm) plot for tensions of 0 (red), 20 (orange), 30 (yellow), and 40 (green) kJ/mol/nm. Dashed line indicates the maximum hydrogen bonding distance.

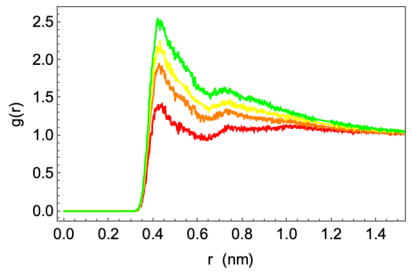

Figure 12. Average carbon-to-carbon $g(r)$ vs r (nm) plots for tensions of 0 (red), 20 (orange), 30 (yellow), and 40 (green) kJ/mol/nm.

Evidently, the probability of finding carbons close to each other increases markedly as tension increases, reflecting the incipient phase separation.

CONCLUSIONS

In this paper, we investigate the phase behavior of PEO solutions under tension, which gives rise to chain confirmations reminiscent of strong flow. Previous MD simulations of PEO in water focus mainly on how changes in hydrogen bonding and polymer configuration qualitatively affect the solubility. Here, we measure the osmotic equation of state using a method recently developed in our group and obtain the effective χ parameter by fitting to the Flory–Huggins equation of state. The evolution of the Flory–Huggins χ parameter with increasing tension quantifies the decreasing solvent quality of water when PEO chains are stretched.

To measure the osmotic equation of state, we use a harmonic potential to pull chains toward the middle of the simulation box, resulting in nonuniform concentration profiles. Analyzing the force balance on the concentration profiles, we obtain $\Pi(\phi)$. To study the effects of tension on phase behavior, we pull on the ends of each chain. Our tension values vary from zero to 40 kJ/mol/nm ≈66.4 pN, which is 17 times the characteristic force $F_c = kT/L_k \approx 4$ pN at which Kuhn segments begin to align. Qualitatively, as pull forces increase, the concentration in the middle of the box increases, reflecting a decrease in solvent quality.

For chain tensions above 20 kJ/mol/nm, water becomes a poor solvent ($\chi > 0.5$) and PEO begins to phase separate. At such tensions, chains are stretched but far from fully aligned. We also find χ modestly increases as the concentration increases, reflecting poorer solvent quality in concentrated solutions.

Our findings appear consistent with previous experimental results. PEO becomes less soluble in water as it is stretched by strong flow[3] and when the polymer concentration of the system increases.[6] Furthermore, structural characterization of simulations of chains under tension but no confining potential are consistent with a decrease in hydrogen bonding and an eventual decrease in solubility as tension on PEO concentration increases.

Our simulation method has two remarkable and convenient features that may on first sight seem too good to be true: (1) we replace a simulation of chains in extensional flow by chains under tension, and (2) we simulate rather short chains. Here, we reflect on why these simplifications are justified.

Of course, chain length matters for rheology, controlling whether a chain is long enough to be stretched at a given shear or extension rate. However, polymer–solvent interactions and hence χ are local properties, which we assert can be inferred from studies on quite short chains.

Extension rates sufficient to stretch long entangled chains are many orders of magnitude lower than local relaxation rates for configurations in water. Thus, we expect PEO strands stretched by flow to be surrounded by water molecules in locally equilibrated configurations. Hence, short chains under tension in quiescent fluid are locally representative of strands in long chains stretched by extensional flow.

Thermodynamically, demixing from a poor solvent is largely independent of chain length since for all but the shortest chains, entropy of mixing is weak on a per-monomer basis, and chains separate as soon as interactions become unfavorable.

Finally, effects of chain end groups on strain-induced phase separation are clearly weak for long PEO chains, such as those used by Ryan and Mykhaylyk. In our simulations, we use methyl-terminated chains to avoid being confounded by chain-end effects, which could be noticeable for our short chains.

APPENDIX

GROMACS pulling options are versatile but sometimes confusing. For completeness, we include below examples of the pulling options used for applying the harmonic potential to every oxygen atom in every PEO chain (Table 1) and for applying equal and opposite forces to the ends of every PEO chain (Table 2).

AUTHOR INFORMATION

Corresponding Author

Scott T. Milner − *Pennsylvania State University, University Park 16802, Pennsylvania, United States;* orcid.org/0000-0002-9774-3307; Email: stm9@psu.edu

Author

Wezi D. Mkandawire − *Pennsylvania State University, University Park 16802, Pennsylvania, United States*

Complete contact information is available at: https://pubs.acs.org/10.1021/acs.macromol.0c02334

Notes

The authors declare no competing financial interest.

ACKNOWLEDGMENTS

We thank the National Science Foundation for funding from DMR-1905632.

REFERENCES

(1) Allen, C.; Maysinger, D.; Eisenberg, A. Nano-engineering block copolymer aggregates for drug delivery. *Colloids Surf., B* **1999**, *16*, 3–27.

(2) Kwon, G. S.; Okano, T. Polymeric micelles as new drug carriers. *Adv. Drug Delivery Rev.* **1996**, *21*, 107−116.
(3) Dunderdale, G. J.; Davidson, S. J.; Ryan, A. J.; Mykhaylyk, O. O. Flow-induced crystallisation of polymers from aqueous solution. *Nat. Commun.* **2020**, *11*, 3372.
(4) Dormidontova, E. E. Role of Competitive PEO−Water and Water−Water Hydrogen Bonding in Aqueous Solution PEO Behavior. *Macromolecules* **2002**, *35*, 987−1001.
(5) Bekiranov, S.; Bruinsma, R.; Pincus, P. Solution behavior of polyethylene oxide in water as a function of temperature and pressure. *Phys. Rev. E: Stat. Phys., Plasmas, Fluids, Relat. Interdiscip. Top.* **1997**, *55*, 577−585.
(6) Bae, Y. C.; Shim, J. J.; Soane, D. S.; Prausnitz, J. M. Representation of vapor−liquid and liquid−liquid equilibria for binary systems containing polymers: Applicability of an extended flory−huggins equation. *J. Appl. Polym. Sci.* **1993**, *47*, 1193−1206.
(7) Smith, G. D.; Bedrov, D.; Borodin, O. Molecular Dynamics Simulation Study of Hydrogen Bonding in Aqueous Poly(Ethylene Oxide) Solutions. *Phys. Rev. Lett.* **2000**, *85*, 5583−5586.
(8) Donets, S.; Sommer, J.-U. Molecular Dynamics Simulations of Strain-Induced Phase Transition of Poly(ethylene oxide) in Water. *J. Phys. Chem. B* **2018**, *122*, 392−397.
(9) Gillespie, C.; Milner, S. T. Using osmotic pressure simulations to test potentials for ions. *Soft Matter* **2020**, *16*, 9816.
(10) Flory, P. J. *Principles of Polymer Chemistry*; Cornell University Press: Ithica, New York, 1953.
(11) Humphrey, W.; Dalke, A.; Schulten, K. VMD: Visual molecular dynamics. *J. Mol. Graphics* **1996**, *14*, 33−38.
(12) Brooks, B. R.; Bruccoleri, R. E.; Olafson, B. D.; States, D. J.; Swaminathan, S.; Karplus, M. CHARMM: A program for macromolecular energy, minimization, and dynamics calculations. *J. Comput. Chem.* **1983**, *4*, 187−217.

https://doi.org/10.1021/acs.macromol.0c02334
Macromolecules 2021, 54, 3613−3619